

ACEMD : Accelerating bio-molecular dynamics in the microsecond time-scale

M. J. Harvey,^{1,*} G. Giupponi,^{2,†} and G. De Fabritiis^{3,‡}

¹*Information and Communications Technologies,
Imperial College London, South Kensington, London, SW7 2AZ, UK*

²*Department de Fisica Fundamental, Universitat de Barcelona,
Carrer Martí i Franques 1, 08028 Barcelona, Spain*

³*Computational Biochemistry and Biophysics Lab (GRIB-IMIM),
Universitat Pompeu Fabra, Barcelona Biomedical Research Park (PRBB),
C/ Doctor Aiguader 88, 08003 Barcelona, Spain*

Abstract

The high arithmetic performance and intrinsic parallelism of recent graphical processing units (GPUs) can offer a technological edge for molecular dynamics simulations. ACEMD is a production-class bio-molecular dynamics (MD) simulation program designed specifically for GPUs which is able to achieve supercomputing scale performance of 40 nanoseconds/day for all-atom protein systems with over 23,000 atoms. We illustrate the characteristics of the code, its validation and performance. We also run a microsecond-long trajectory for an all-atom molecular system in explicit TIP3P water on a single workstation computer equipped with just 3 GPUs. This performance on cost effective hardware allows ACEMD to reach microsecond timescales routinely with important implications in terms of scientific applications.

I. INTRODUCTION

The simulation of mesoscopic scales (microseconds to milliseconds) of macromolecules continues to pose a challenge to modern computational biophysics. Whilst the fundamental thermodynamic framework behind the simulation of macromolecules is well characterised, exploration of biological time scales remains beyond the computational capacity routinely available to many researchers. This has significantly inhibited the widespread use of molecular simulations for *in silico* modelling and prediction¹.

Recently, there has been a renewed interest in the development of molecular dynamics simulation techniques. D. E. Shaw Research² has fostered several significant algorithmic improvements including mid-point³ and neutral-territory methods⁴ for the summation of non-bonded force calculations, a new molecular dynamics package called Desmond⁵ and Anton², a parallel machine for molecular dynamics simulations that uses specially-designed hardware. Other parallel MD codes, such as Blue matter⁶, NAMD⁷ and Gromacs⁸, have been designed to perform parallel MD simulations across multiple independent processors, but latency and bandwidth limitations in the interconnection network between processors reduces parallel scaling unless the size of the simulated system is increased with processor count. Furthermore, dedicated, highly-parallel machines are usually expensive and not reservable for long periods of time due to cost constraints and allocation restrictions.

A further line of development of MD codes consists of using commodity high performance accelerated processors¹. This approach has become an active area of investigation, particularly in relation to the Sony-Toshiba-IBM Cell processor⁹ and graphical processing units (GPUs). Recently, De Fabritiis⁹ implemented an all-atom biomolecular simulation code, CellMD, targeted to the architecture of the Cell processor (contained within the Sony Playstation3) that reached a sustained performance of 30 Gflops with a speedup of 19 times compared to the single CPU version of the code. At the same time, a port of the Gromacs code for implicit solvent models¹⁰ was developed and used by the Folding@home distributed computing project¹¹ on a distributed network of Playstation3s. Similarly, CellMD was used in the PS3GRID.net project¹² based on the BOINC platform¹³ moving all-atom MD applications into a distributed computing infrastructure.

Pioneers in the use of GPUs for production molecular dynamics¹¹ had several limitations imposed by the restrictive, graphics-orientated OpenGL programming model¹⁴ then

available. In recent years, commodity GPUs have acquired non-graphical, general-purpose programmability and have undergone a doubling of computational power every 12 months, compared to 18 – 24 months for traditional CPUs¹. Of the devices currently available on the market, those produced by Nvidia offer the most mature programming environment, the so-called compute unified device architecture (CUDA)¹⁵, and have been the focus of the majority of investigation in the computational science field.

Several groups have lately shown results for MD codes which utilise CUDA-capable GPUs. Stone *et al*¹⁶ demonstrated the GPU-accelerated computation of the electrostatic and van der Waals forces, reporting a 5.4 times speed-up with respect to a conventional CPU. Meel *et al*¹⁷ described an implementation for simpler Lennard-Jones atoms which achieved a net speedup of up to 40 times over a conventional CPU. Unlike the former, the whole simulation is performed on the GPU. Recently, Phillips *et al* have reported experimental GPU-acceleration of NAMD¹⁸ yielding speedups of up to 7 times over NAMD 2.6.

In this work, we report on a molecular dynamics program called ACEMD which is optimised to run on Nvidia GPUs and which has been developed with the aim of advancing the frontier of molecular simulation towards the ability to routinely perform microsecond-scale simulations. ACEMD maximises performance by running the whole computation on the GPU rather than offloading only selected computationally-expensive parts. We have developed ACEMD to implement all features of a typical MD simulation including those usually required for production simulations such as particle-mesh Ewald (PME¹⁹) calculation of long range electrostatics, thermostatic control and bond constraints. The default force-field format used by ACEMD is CHARMM²⁰ although the code can also use the Amber99²¹ force field once converted to the format of the former²². ACEMD also provides a scripting interface to control and program the molecular dynamics run to perform complex protocols like umbrella sampling, steered molecular dynamics and sheared boundary conditions.

II. GPU ARCHITECTURE

The G80 and subsequent G200 generations of Nvidia GPU architectures are designed for data-parallel computation, in which the same program code is executed in parallel on many data elements. The CUDA programming model, an extended C-like language for GPUs, abstracts the implementation details of the GPU so that the programmer may easily write code

that is portable between current and future GPUs. Nvidia GPU devices are implemented as a set of multiprocessor (MP) devices, each of which is capable of synchronously executing 32 program threads in parallel (called warp) and managing up to 1024 concurrently (Figure 1). Current Nvidia products based on these devices are able to achieve up to 933 Gflops in single precision. By comparison, a contemporary quad core Intel Xeon CPU is capable of approximately 54 Gflops²³. A brief comparison of the characteristics of these devices is given in Table I. Each MP has a set of 32 bit registers, which are allocated as required to individual threads, and a region of low-latency shared memory that is accessible to all threads running on it. The MP is able to perform random read/write access to external memory. Access to this global memory is uncached and so incurs the full cost of the memory latency (up to 400 cycles). However, when accessed via the GPU’s texturing units, reads from arrays in global memory are cached, mitigating the impact of global memory access for certain read patterns. Furthermore, the texture units are capable of performing linear interpolation of values into multidimensional (up to 3D) arrays of floating point data.

Whilst the older G80 architecture supported only single-precision IEEE-754 floating point arithmetic, the newer G200 design also supports double-precision arithmetic, albeit at a much lower relative speed. The MP has special hardware support for reciprocal square root, exponentiation and trigonometric functions, allowing these to be computed with low latency but at the expense of slightly reduced precision.

Program fragments written to be executed on the GPU are known as *kernels* and are executed in *blocks*. Each block consists of multiple instances of the kernel, called *threads*, which are run concurrently on a single multiprocessor. The number of threads in a block is limited by the resources available on the MP but multiple blocks may be grouped together as a *grid*. The CUDA runtime, in conjunction with the GPU hardware itself, is responsible for efficiently scheduling the execution of a grid of blocks on available GPU hardware. CUDA does not presently provide a mechanism for transparently using multiple GPU devices for parallel computation. For full details of the CUDA environment, the reader is referred to the SDK documentation²⁴.

	Tesla C870 (G80)	Tesla C1060 (G200)	Intel Xeon 5492
Cores	128	240	4
Clock (GHz)	1.350	1.296	3.4
Mem bandwidth (MB/s)	77	102	21
Gflops	512 (sp)	933 (sp) 78 (dp) 54 (dp)	
Power (W)	171	200	150
Year	2007	2008	2008

TABLE I: Summary of characteristics of first and second generation Nvidia GPU compute devices, with a contemporary Intel Xeon shown for comparison. Data taken from manufacturers' data sheets. (sp stands for single precision and dp for double precision).

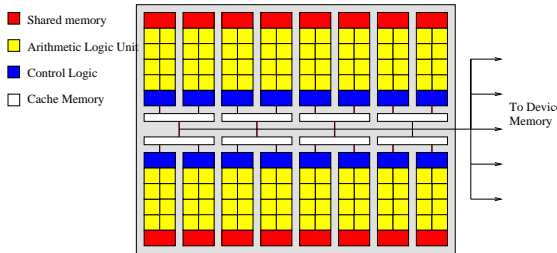


FIG. 1: Nvidia GPU design is based around an 8 core single program, multiple data (SPMD) processor. Each core has local storage provided by the register file and access to a shared memory region. Read/write access to the main device memory is uncached, except for some specific read-only access modes. The above figure represents the G80-series device with 16 such processors, whilst the contemporary G200 contains 30 (Tesla C1060, GTX280), giving 240 cores.

III. MOLECULAR DYNAMICS ON THE GPU

ACEMD implements all features of an MD simulation on a CUDA-compatible GPU device, including those usually required for production simulations in the NVT ensemble (*ie* bonded and non-bonded force term computation, velocity-Verlet integration, Langevin thermostatic control, smooth Ewald long range electrostatics (PME)^{19,25} and hydrogen bond constraints). Also implemented is the hydrogen mass repartitioning scheme described in

Ref.²⁶ and used for instance in codes such as Gromacs, which allows an increased timestep of up to 4 fs. The code does not presently contain a barostat, so simulations in the NPT ensemble are not possible. However, it is noted that with large molecular systems, changes in volume due to the pressure control are very limited after an initial equilibration making NVT simulations viable for production runs. ACEMD supports the CHARMM27 force field and Amber99 in CHARMM format²², PDB, PSF and DCD file formats²⁷ as well as steered molecular dynamics²⁸, check-pointing and input files compatible with a widely used MD codes such as NAMD.

The computation of the non-bonded force terms dominates the computational cost of MD simulations and it is therefore important to use an efficient algorithm. As in^{9,17}, we implement a cell-list scheme in which particles are binned according to their co-ordinates. On all-atom biomolecular systems a cutoff of $R = 12 \text{ \AA}$ with bins $R/2$ gives an average cell population of approximately 22 atoms. This is comparable to the warp size of 32 for current Nvidia GPUs. In practice, however, transient density fluctuations can lead to the cell population exceeding the warp size. Consequently, the default behaviour of ACEMD is to assume a maximum cell population of 64. The code may also accommodate a bin size of R for coarse-grained simulations. The cell-list construction kernel processes one particle per thread, with each thread computing the cell in which its atom resides. To permit concurrent manipulation of a cell-list array, atomic memory operations are used.

The non-bonded force computation kernel processes a single cell per thread block, computing the full Lennard-Jones and electrostatic force on each particle residing within it. All of the cells within R of the current cell (including a copy of the cell itself) are loaded into shared memory in turn. Each thread then computes the force on its particle by iterating over the array in shared memory. In contrast to CPU implementations, reciprocal forces are not stored for future use (*ie* the force term F_{ij} is not saved for reuse as F_{ji}), because of the relatively high cost of global memory access. The texture units are used to assist the calculation of the electrostatic and van der Waals terms by providing linearly interpolated values for the radial components of those functions from lookup tables. The interpolation error is low and does not affect the energy conservation properties of NVE simulations. In production runs (Figure 2), the relative force error compared to a reference simulation performed in double precision is consistently less than 10^{-4} , below the 10^{-3} error considered the maximum acceptable for biomolecular simulations⁵. Particle-mesh Ewald (PME)²⁵

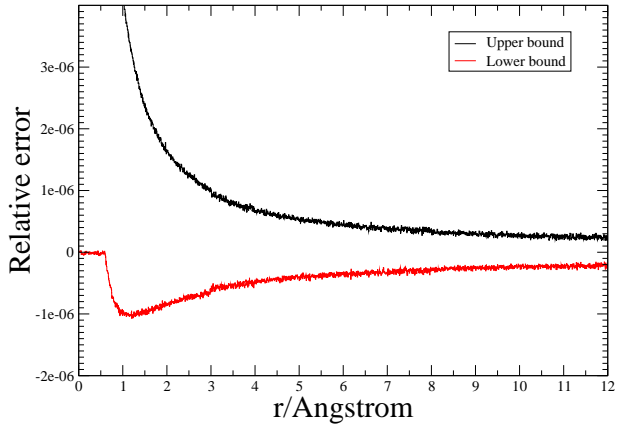


FIG. 2: The bounds (running average) of the relative error $\frac{E_{\text{interp}} - E_{\text{calc}}}{E_{\text{calc}}}$ between directly calculated and lookup table (linear interpolation, $n = 4096$) values of the van der Waals potential. Error has a period of $\frac{R_{\max}}{n}$

evaluation of long-range electrostatics is also supported by a dedicated kernel. All parts of this computation are performed on the GPU, with support from the Nvidia FFT library²⁹. For PME calculations, a cutoff of $R = 9.0 \text{ \AA}$ is considered to provide sufficient accuracy, permitting the maximum cell population to be limited to 32 atoms.

To support CHARMM and AMBER force fields, it is necessary to selectively exclude or scale non-bonded force terms between atoms that share an explicit bond term. The indices of excluded and 1-4 scaled pairs are stored in bitmaps, allowing any pair of particles with indices i, j such that $|i - j| \leq 64$ to be excluded or scaled¹⁶. Exclusions with larger index separations are also supported in order to accommodate, for example, disulphide bonds but the additional book-keeping imposes a minor reduction in performance. Because the atoms participating in bonded terms are spatially localised, it is necessary only to make exclusion tests for interactions between adjacent cells despite, for cells of $R/2$, the interaction halo being two cells thick. A consequent optimisation is the splitting of the non-bonded force kernel into two versions, termed *inner* and *outer*, which respectively include and omit the test.

Holonomic bond constraints are implemented using the M-shake algorithm³⁰ and RAT-TLE for velocity constraints³¹ within the velocity Verlet integration scheme³². M-shake is

Timestep (fs)	constraints	HMR	$K_bT/\text{ns/dof}$
1	no	no	0.00021
2	yes	no	-0.00082
4	yes	yes	-0.00026

TABLE II: Energy change in the NVE ensemble per nanosecond per degrees of freedom (dof) in K_bT units for dihydrofolate reductase (DHFR) using different integration timesteps, constraints and hydrogen mass repartitioning (HMR) schemes.

an iterative algorithm and, in order to achieve acceptable convergence it is necessary to use double precision arithmetic (a capability available only on G200/architecture 1.3 class devices). For the pseudo-random number source for the Langevin thermostat we use a Mersenne twister kernel, modified from the example provided in the CUDA SDK.

IV. SINGLE-PRECISION FLOATING-POINT ARITHMETIC VALIDATION

ACEMD uses single-floating point arithmetic because the performance of GPUs on single precision is much higher than double precision and the limitation of single floating-point can be controlled well for molecular dynamics^{8,9}. Nevertheless, we validate in this section the conservation properties of energy in a NVT simulation using rigid and harmonic bonds, as constraints have shown to be more sensitive to numerical precision. Potential energies were checked against NAMD values for the initial configuration of a set of systems, including disulphide bonds, ionic system, protein and membranes, in order to verify the correctness of the force calculations by assuring that energies were identical within 6 digits. The Langevin thermostat algorithm was tested for three different damping frequencies $\gamma = 0.1, 0.5, 1.0$ with a reference temperature of $T = 300K$ and both with and without constraints.

The test simulations consist of nanosecond runs of dihydrofolate reductase (DHFR) joint AMBER-CHARMM benchmark with volume $62.233 \times 62.233 \times 62.233 \text{ \AA}^3$ (a total of 23,558 atoms)⁵. Each simulation system was firstly equilibrated at a temperature of $T = 300K$ and then relaxed in the NVE ensemble. A reference simulation with harmonic bonds and timestep $dt = 1 \text{ fs}$ was also performed, as well as simulations with $dt = 2 \text{ fs}$ using rigid constraints and with $dt = 4 \text{ fs}$ with rigid constraints and hydrogen mass repartitioning (HMR)

with a factor 4.0, as in³³. In Table II, we show the energy change per nanosecond per degrees of freedom in units of K_bT , which is similar with other single and double precision codes MD³⁴. We note that even when using bigger timesteps and a combination of M-shake and hydrogen mass repartitioning, energy conservation is reasonably good, and much slower than the timescale at which the thermostat would act. Hydrogen mass repartitioning is an elegant way to increase the timestep up to 4 fs by increasing the momentum of inertia of groups of atoms bonded to hydrogen atoms. The mass of the bonded heavy atoms to hydrogens is repartitioned among hydrogen atoms, leaving the total mass of the system unchanged. As individual atom masses do not appear in the expression for the equilibrium distribution, this repartition affects only the dynamic properties of the system not the equilibrium distribution. Following²⁶, a factor 4 for hydrogens affects only marginally the diffusion and viscosity of TIP3P water (which is in any case inaccurate when compared to experimental data). A similar speed up could also be obtained by using a smaller timestep with the evaluation of the long range electrostatic terms every other timestep.

We also validated the implementation of the PME algorithm to compute long range electrostatics forces. We run a set of simulations using different timesteps and algorithms as above ($dt = 1, 2$ fs rigid bonds , $dt = 4$ fs rigid bonds and hydrogen mass repartitioning) on a $40.5 \times 40.5 \times 40.5\text{\AA}^3$ box of 1 M solution of NaCl in water (6461 atoms), as in³⁵. PME calculations were performed with a $64 \times 64 \times 64$ grid size. Two simulations of the same system were used as reference, one with Gromacs⁸ with PME as in³⁵, and the other using ACEMD with an electrostatic cutoff of 12 Å without PME. We calculated the Na-Na pair distribution function $g(r)$ in Figure 3 in order to compare the simulation results for different simulations and methods, as from³⁵ Na-Na $g(r)$ results as the quantity more sensitive to different methods for electrostatics calculations. We note that for all integration timesteps used, ACEMD agrees well with the reference simulation made with Gromacs. In addition, using PME gives consistently better results than using a 12 Å cutoff for this simple homogeneous system, as expected. A direct validation of the pair distribution function with the hydrogen mass repartitioning method is also shown in Fig. 3 comparing the $g(r)$ for timestep equal 1, 2, 4.

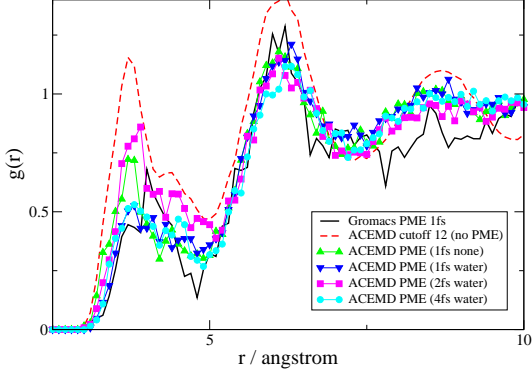


FIG. 3: Plot of Na-Na pair distribution functions for a 1M NaCl water box as in³⁵.

Program	CPU Cores & GPUs	ms/step
ACEMD	1 CPU, 1 GPU (240 cores)	17.55
ACEMD	3 CPU, 3 GPU (720 cores)	7.56
NAMD2.6	128 CPU (64 nodes)	9.7
NAMD2.6	256 CPU (128 nodes)	7.0
Desmond	32 CPU (16 nodes)	11.5
Desmond	64 CPU (32 nodes)	6.3
Gromacs4	20 CPU (5 nodes)	7

TABLE III: Performance of ACEMD on the DHFR benchmark. GPUs are Nvidia GTX 280. NAMD, Desmond and Gromacs performances are indicative of the orders of magnitude speed-up obtained with GPUs and ACEMD as they are all performed on different CPU systems (from Refs^{5,8}, Gromacs figures interpolated from Figure 6 of⁸).

V. PERFORMANCE

The current implementation of ACEMD is parallelized in a task parallel manner designed to scale across just 3 GPUs attached to a single host system. A simple force-decomposition scheme³⁶ is used, in which each GPU computes a subset of the force terms. These force terms are summed on by the host processor and the total force matrix transferred back to each GPU which then perform integration of the whole system. ACEMD dynamically load-balances the computation across the GPUs. This allows the simulation of heterogeneous molecular

Program	CPU Cores & GPUs	ms/step
ACEMD	1 CPU, 1 GPU (1 node)	73.4
ACEMD	3 CPU, 3 GPU (1 node)	32.5
NAMD	4 CPU, 4 GPU (1 node)	87
NAMD	16 CPU, 16 GPU (4 nodes)	27
NAMD	60 CPU (15 nodes)	44

TABLE IV: Performance of ACEMD and NAMD on the apoA1 benchmark. ACEMD run using Nvidia GTX 280 GPUs ($R = 9\text{\AA}$, PME every step), NAMD ($R = 12\text{\AA}$, PME every 4 steps) run with G80-series GPUs (approximately half as fast) NAMD performance data taken from¹⁸.

systems and also accommodates variation due to host system architecture (for example, different speed GPUs or GPU-host links). For simulations requiring PME, a heterogeneous task decomposition is used, with a subset of GPUs dedicated to PME computation.

The performance benchmark is based on the DHFR molecular system with a cutoff of $R = 9\text{\AA}$, switched at 7.5\AA , $dt = 4$ fs, PME for long range electrostatic with $64 \times 64 \times 64$ grid size and fourth order interpolation, M-shake constraints for hydrogen bonds and hydrogen mass repartitioning. All simulations were run on a PC equipped with 4 Nvidia GPU GTX 280 cards at 1.3GHz (just 3 GPUs used for these tests), a quad core AMD Phenom processor (2.6GHz), MSI board with AMD790 FX chipset, 4GB RAM running Fedora Core 9, CUDA toolkit 2.0 and the Nvidia graphics driver 177.73. Performance results reported in Table III indicates that ACEMD requires 17.55 ms per step with the DHFR system and 7.56 ms per step when run in parallel over the 3 GPUs. As expected by the simple task decomposition scheme, ACEMD achieves a parallel efficiency of 2.3 over 3 GPUs. Further device-to-device communication directives may substantially improve these results as they will enable the use of spatial-decomposition parallelisation strategies, such as neutral territory (NT) schemes⁴. Comparing directly the maximum performance of ACEMD on the DHFR system with results of various MD programs from Ref.⁵ we obtain a performance approaching that of 256 CPU cores using NAMD and 64 using Desmond on a cluster with fast interconnect. Using hydrogen mass repartitioning and a time step of 4 fs integration timestep it is possible to simulate trajectories of over 45 ns per day with 3 GPUs and almost

20 nanosecond per day with a single GPU. An highly optimised code such as Gromacs⁴ requires only 20 CPU cores to deliver similar performance to 3 GPUs on DHFR⁸, but the calculations are not identical as, for instance, there are several optimisations applied to water.

Representative performance data for ACEMD and the the GPU-accelerated version of NAMD¹⁸ for the apoA1 benchmark system (92,224 atoms) is given in Table IV. Differences between the simulation and hardware configurations prevent a direct comparison but it is salient to note that because the enhanced NAMD retains the spatial decomposition parallelism it is able to scale across multiple GPU-equipped hosts, whilst ACEMD is designed for optimal performance on a small number of GPUs.

VI. MICROSECOND SIMULATIONS ON WORKSTATION HARDWARE

To provide a direct demonstration that molecular simulations have now entered the microsecond regime *routinely* we perform a microsecond long trajectory performed on a workstation-class PC. We use for this task the chicken Villin headpiece (HP-35) structure, one of the smallest polypeptides with a stable globular structure comprising three alpha-helices placed in a "U"-shaped form, as shown in Figure 4c. Due to its small size, it is commonly used as a subject in long molecular simulations for folding studies, for instance³⁷, which uses highly parallel distributed-computing to compute many trajectories to fully sample the phase space of the folding process. Alternatively, mutanogenesis studies on folding³⁸ have been performed using biased methods to accelerate the sampling.

The Villin headpiece (PDB:1YRF) was fully solvated in TIP3P water and Na-Cl at 150mM (a total of 13701 atoms) using the program VMD³⁹ and the CHARMM force-field. The system was then equilibrated at 300K and 1atm for 10ns using NAMD2.6⁷ with a cutoff of 9 Å, PME with a $48 \times 48 \times 48$ grid, constraints for all H bond terms and a timestep of 2fs. Simulations with ACEMD were performed using an NVT ensemble, hydrogen mass repartitioning and timestep of 4fs. Starting from the final equilibrium configuration of NAMD, we run ACEMD at 450K for 40 ns until the system was completely unfolded (movie available at⁴⁷). The resulting extended configuration (Figure 4b) was then used as the starting point of a microsecond long single trajectory at a temperature of 305K. Figure 4a, shows the RMSD of the backbone of the protein along the trajectory. The minimum

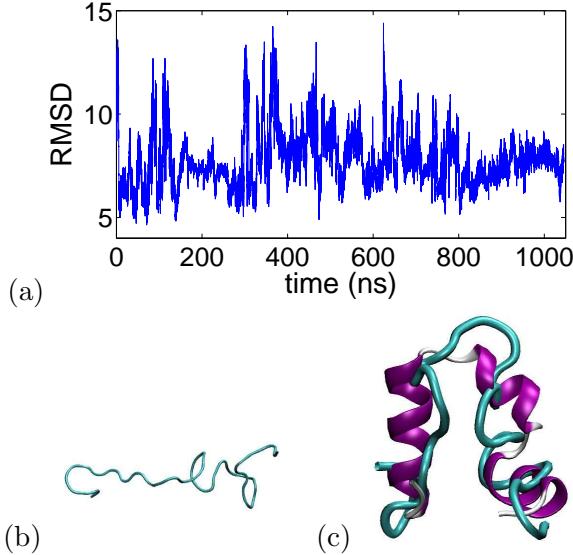


FIG. 4: (a) The RMSD of the backbone of the protein during the microsecond simulation starting from the unfolded configuration (b) of the Villin system with 13,701 atoms (TIP3P water not shown for clarity). Within our simulation window the minimum RMSD was 4.87 Å for which the resulting best structure is overlapped with the crystal structure in (c).

RMSD was 4.87. The protein seems to sample quite often the overall shape of the crystal structure yet not converge towards it (Figure 4c). As this structure is expected to fold in 4-5 microseconds, we plan to extend the dynamics in the future along with any newer and faster version of ACEMD (for instance using the new Nvidia GTX295 cards or, more likely, quad GPU Tesla S1075 units). An important consideration with regards to the force-field: with molecular simulations approaching the microseconds, it is clear that the accuracy of the force-fields will become more and more important. In particular, this system has shown to be very sensitive to the force-field used³⁸ (CHARMM seems to converge poorly towards the folded structure).

The production run on a PC equipped with ACEMD and 3 Nvidia GPUs (720 cores) required approximately 15 days (66 nanoseconds/day) (see Table V) and probably represents the limit for current hardware and software implementation, while 5 microseconds should be obtainable in the near future using a 4-way GTX295 based system with 8 GPU cores. Using currently-available commodity technology, the construction of computer systems with up to 8 directly-attached GPUs has been demonstrated^{48,16}. GPUs attach to the host system using the industry-standard PCI-Express interface⁴⁰. This interface is characterised by a

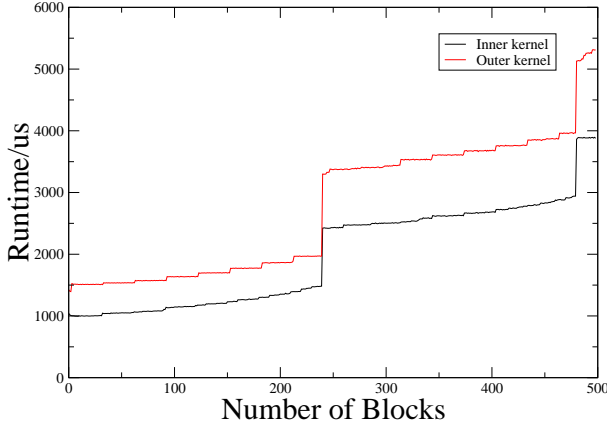


FIG. 5: Runtime for the non-bonded force calculation kernels on a water box as a function of the number of blocks per invocation and run on an Nvidia Tesla C1060 GPU (30 multiprocessors). The inner and outer kernels both have an occupancy of 8 blocks/multiprocessor. Blocks are distributed across multiprocessors, with the small step increases indicating an increment in the number of simultaneous blocks. The large steps indicate the device is fully populated with blocks and that some MPs must sequentially process further block. Optimal resource usage occurs immediately before these steps. The effect of gradual divergence between multiprocessors is seen as block count increases. The minimum runtime for the fully parallel case would be 3.4 ms.

System	CPUs & GPUs	ns/day
DHFR	1 CPU, 1 GPU (240 cores)	19.7
DHFR	1 CPU, 3 GPUs (720 cores)	45.7
apoA1	1 CPU, 1 GPU (240 cores)	4.6
apoA1	3 CPU, 3 GPUs (720 cores)	10.6
Villin	3 CPU, 3 GPUs (720 cores)	66.0

TABLE V: Performance of ACEMD on the DHFR, apoA1 benchmark and Villin test on 1 and 3 GPUs up to 720 cores. ACEMD run using Nvidia GTX 280 GPUs on a real production runs ($R = 9\text{\AA}$, PME every step, time step 4 fs, constraints and langevin thermostat).

bandwidth comparable to that of main system memory (up to 8GB/s for 16 lane PCIe 2.0 links typically used by graphics cards) but with a relatively higher latency.

The GPU resource requirements of the non-bonded kernel make it possible for up to 8 independent blocks to be processed simultaneously per multiprocessor. The limit of parallelization for the execution of the non-bonded kernel occurs when all blocks may be processed simultaneously by the available multiprocessors. Thus, for instance, a cubic simulation box with $l = 66\text{\AA}$ and cell size 6\AA would scale over 167 multiprocessors (1336 cores), or 6 G200-class GPUs. Figure 5 shows the runtime of the inner and outer non-bonded kernels on a water box as a function of block count per kernel invocation. The minimum computation time for the fully-parallel case would be 3.4 ms/step on current hardware. To further improve performance, optimisation of the kernel or further subdivision of the computation would be required.

VII. CONCLUSIONS

We have presented a molecular dynamics application, ACEMD, designed to reach the microsecond timescale even on cost-effective workstation hardware using the computational power of GPUs. It supports the CHARMM27 force field and Amber force field in CHARMM format and is therefore suitable for use in modelling biomolecular systems. The ability to model these systems for tens of nanoseconds per day makes it feasible to perform simulations of up to the microsecond scale over the course of a few weeks on a suitable GPU-equipped machine. Calculations lasting a few weeks are perfectly reasonable tasks on workstation-class computers equipped with single or multiple GPUs. The current implementation limits the number of atoms to a maximum of 250,000 atoms which could be extended.

ACEMD has been extensively tested since August 2008 through its deployment on the several thousand GPU-equipped PCs which participate in the volunteer distributed computing project GPUGRID.net⁴¹, based on the Berkeley Open Infrastructure for Networked Computing (BOINC)⁴² middleware. At the time of writing, GPUGRID.net delivers over 30 Tflops of sustained performance⁴³, and is thus one of the largest distributed infrastructures for molecular simulations, producing thousands of nanosecond long trajectories per day for high-throughput molecular simulations, for instance for accurate virtual screening⁴⁴.

The current implementation of ACEMD limits its parallel performance to just 3 GPUs

due to a simple task parallelization. We plan to extend the use of ACEMD on more GPUs, but keeping the focus on scalability, so small numbers of GPUs (1-32). Ideally the optimal system for ACEMD would rely on a single node attached to a large number of GPUs via individual PCIe expansion slots in order to take advantage of the large interconnect bandwidth. ACEMD would potentially scale very well on such machine due to the fact that it is entirely executing on the GPU devices, obtaining CPU loads within just 5%. For efficient scaling across a GPU-equipped cluster, we anticipate that a re-factoring of the parallelisation scheme to use a spatial decomposition method⁴ would be necessary, moving away from the simple task parallelisation used in this work. Possible future developments also include support of forthcoming programming languages for GPUs, for example OpenCL⁴⁵, a development library which is intended to provide a hardware-agnostic, data-parallel programming model. Whilst GPU devices are commonly present in desktop and workstation computers for graphics purposes, as accelerator processors they have yet to become routinely integrated components of the compute cluster systems typically used for high-performance computing (HPC) systems. GPU workstations, such as the one used in this work are readily available, while GPU clusters are slowly appearing⁴⁹. In order to scale efficiently, low-latency, high-bandwidth communications between nodes is necessary. For example, Bowers *et al*⁵, describe the scaling of the Desmond MD program over an Infiniband⁴⁶ network and demonstrate improved scaling when using custom communications routines tailored to the requirements of the algorithm and the capabilities of the network technology.

Accelerated molecular dynamics on GPUs as provided by ACEMD should be of wide interest to a large number of computational scientists as it provides performance comparable to that achievable on standard CPU supercomputers in a laboratory environment. Even research groups that have routine access supercomputing time might find useful the ability to run simulations locally for longer time windows and with added flexibility.

Acknowledgements. This work was partially funded by the HPC-EUROPA project (R113-CT-2003-506079). GG acknowledges support from the Marie Curie Intra-European Fellowship (IEF). GDF acknowledges support from the Ramon y Cajal scheme and also from the EU Virtual Physiological Human Network of Excellence. We gratefully acknowledge the advice of Sumit Gupta (Nvidia), Acellera Ltd (<http://www.acellera.com>) for use of their resources and Nvidia Corporation (<http://www.nvidia.com>) for their hardware donations.

We thank Ignasi Buch for help in debugging the software.

* Electronic address: m.j.harvey@imperial.ac.uk

† Electronic address: giupponi@ffn.ub.es

‡ Electronic address: gianni.defabritiis@upf.edu

¹ Giupponi, G.; Harvey, M. J.; de Fabritiis, G. *Drug Discovery Today* **2008**, *13*, 1052.

² Shaw, D. E. Anton, a Special-Purpose Machine for Molecular Dynamics Simulation. In *Proceedings of the 34th annual international symposium on Computer architecture*; : , 2007.

³ Bowers, K. J.; Dror, R. O.; Shaw, D. E. *J. Chem. Phys* **2006**, *24*, 184109.

⁴ Bowers, K. J.; Dror, R. O.; Shaw, D. E. *J. Phys.: Conf. Series* **2005**, *16*, 300-304.

⁵ Bowers, K. J.; Chow, E.; Xu, H.; Dror, R. O.; Eastwood, M. P.; Gregersen, B. A.; Klepeis, J. L.; Kolossvary, I.; Moraes, M. A.; Sacerdoti, F. D.; Salmon, J. K.; Shan, Y.; Shaw, D. E. Scalable Algorithms for Molecular Dynamics Simulations on Commodity Clusters. In *Proceedings of SuperComputing 2006, Tampa, US, 11-17th November*; : , 2006.

⁶ Fitch, B.; Rayshubskiy, A.; Eleftheriou, M.; Ward, T.; Giampapa, M.; Pitman, M.; Germain, R. *IBM RC23956, May* **2006**, *12*.

⁷ Phillips, J. C.; Braun, R.; Wang, W.; Gumbart, J.; Tajkhorshid, E.; Villa, E.; Chipot, C.; Skeel, R. D.; Kale, L.; Schulten, K. *J. Comp. Chem.* **2005**, *26*, 1781-1802.

⁸ Hess, B.; Kutzner, C.; van der Spoel, D.; Lindahl, E. *J. Chem. Theor. and Comp.* **2008**, *4*, 435-447.

⁹ De Fabritiis, G. *Comp. Phys. Commun.* **2007**, *176*, 600.

¹⁰ Luttmann, E.; Ensign, D.; Vaidyanathan, V.; Houston, M.; Rimon, N.; Oland, J.; Jayachandran, G.; Friedrichs, M.; Pande, V. *J Comput Chem* **2008**, *30*, 268.

¹¹ Folding@home <http://folding.stanford.edu>.

¹² Harvey, M. J.; Giupponi, G.; Villà-Freixa, J.; De Fabritiis, G. PS3GRID.NET: Building a distributed supercomputer using the PlayStation 3. In *Distributed & Grid Computing - Science Made Transparent for Everyone. Principles, Applications and Supporting Communities*; : , 2007.

¹³ Berkeley Open Infrastructure for Network Computing <http://www.boinc.berkeley.edu>.

¹⁴ OpenGL, <http://www.opengl.org>.

- ¹⁵ Nickolls, J.; Buck, I.; Garland, M.; Skadron, K. *ACM Queue* **2008**, *6*.
- ¹⁶ Stone, J.; Phillips, J.; Freddolino, P.; Hardy, D.; Trabuco, L.; Schulten, K. *J. Comp. Chem.* **2007**, *28*, 2618-2640.
- ¹⁷ van Meel, J. A.; Arnold, A.; Frenkel, D.; Portegies-Zwart, S. F.; Belleman, R. G. *Mol. Sim.* **2008**, .
- ¹⁸ Phillips, J. C.; Stone, J. E.; Schulten, K. Adapting a message-driven parallel application to GPU-accelerated clusters. In *Proceedings of the 2008 ACM/IEEE Conference on Supercomputing*; IEEE Press: , 2008.
- ¹⁹ Ewald, P. *Ann. Phys.* **1921**, *64*, 253-287.
- ²⁰ MacKerrell *et al*, A. *J. Phys. Chem. B* **1998**, *102*, 3586.
- ²¹ Ponder, J. W.; Case, D. A. *Adv. Prot. Chem.* **2003**, *66*, 27-85.
- ²² Amber forcefield in Charmm format <http://www.glue.umd.edu/~jbklauda/research/download.html>.
- ²³ Dongarra, J. J. “Performance of various computers using standard linear equations software”, Technical Report, Netlib report CS-89-85, 2007.
- ²⁴ “NVIDIA CUDA Compute Unified Device Architecture Programming Guide 2.0”, Technical Report, NVIDIA, 2008.
- ²⁵ Essman, U.; Perera, L.; Berkowitz, M. L.; Darden, T.; Lee, H.; Pedersen, L. G. *J. Chem. Phys.* **1995**, *19*, 8577-8593.
- ²⁶ Feenstra, K. A.; Hess, B.; Berendsen, H. J. C. *J. Comp. Chem* **1999**, *20*, 786.
- ²⁷ David J. Hardy, MDX libraries, <http://www.ks.uiuc.edu/Development/MDTools/namdlite>, University of Illinois at Urbana-Champaign, 2007.
- ²⁸ De Fabritiis, G.; Coveney, P. V.; Villà-Freixa, J. *Proteins* **2008**, .
- ²⁹ Corp, N. “CUDA CUFFT Library, Document PG-00000-003 V2.0”, Technical Report, Nvidia Corp, 2008.
- ³⁰ Kräutler, V.; van Gunsteren, W. F.; Hünenberger, P. H. *J. Comp. Chem* **2001**, *22*, 501-508.
- ³¹ Andersen, H. C. *J. Comp. Phys.* **1983**, *52*, 24-34.
- ³² Verlet, L. *Part. Part. Syst. Charact.* **1967**, *159*, 98.
- ³³ Feenstra, K.; Hess, B.; Berendsen, H. J. *Comp. Chem.* **1999**, *20*, 786-798.
- ³⁴ Lippert, R. A.; Bowers, K. J.; Dror, R. O.; Eastwood, M. P.; Gregersen, B. A.; Klepeis, J. L.; Kolossvary, I. *J. Chem. Phys.* **2007**, *126*, 046101.
- ³⁵ Tironi, I. G.; Sperb, R.; Smith, P. E.; van Gunsteren, W. F. *J. Chem. Phys.* **102**, 5451-5459.

- ³⁶ Plimpton, S.; Hendrickson, B. *J. Comp. Chem.* **1996**, *17*, 326-337.
- ³⁷ Ensign, D.; Kasson, P.; Pande, V. *Journal of Molecular Biology* **2007**, *374*, 806–816.
- ³⁸ Piana, S.; Laio, A.; Marinelli, F.; Van Troys, M.; Bourry, D.; Ampe, C.; Martins, J. *Journal of Molecular Biology* **2008**, *375*, 460–470.
- ³⁹ Humphrey, W.; Dalke, A.; Schulten, K. *J. Mol. Graphics* **1996**, *14*, 33.
- ⁴⁰ “PCI Express Base Specification 2.0”, Technical Report, PCI Special Interest Group, 2007.
- ⁴¹ GPUGRID project, <http://www.gpugrid.net>.
- ⁴² Anderson, D. L. BOINC: A System for Public-Resource Computing and Storage. In *Proceedings of Fifth IEEE/ACM International Workshop on Grid Computing (GRID'04)*; : , 2004.
- ⁴³ Boincstats, <http://www.boincstats.com>.
- ⁴⁴ Random Samples: Play me a Molecule, *Science* **2008**, *321*, 1425.
- ⁴⁵ OpenCL, Khronos Group, <http://www.khronos.org/opencl/>.
- ⁴⁶ “InfiniBand Architecture Specification Volumes 1 & 2”, Technical Report, Infiniband Trade Association, 2004.
- ⁴⁷ <http://www.vimeo.com/2505856>
- ⁴⁸ FASTRA GPU SuperPC, <http://fastra.ua.ac.be/en/index.html>, University of Antwerp (accessed 17th Nov 2008)
- ⁴⁹ Nvidia Tesla-equipped Tsubame cluster, Tokyo Institute of Technology